Published online 8 August 2018

Nucleic Acids Research, 2018, Vol. 46, No. 19 ***10405–10416***
doi: 10.1093/nar/gky696

MIR100 host gene-encoded lncRNAs regulate cell cycle by modulating the interaction between HuR and its target mRNAs

Qinyu Sun[1,†], Vidisha Tripathi[1,*,†], Je-Hyun Yoon[2,3,*], Deepak K. Singh[1], Qinyu Hao[1], Kyung-Won Min[2], Sylvia Davila[2], Richard W. Zealy[2], Xiao Ling Li[4], Maria Polycarpou-Schwarz[5], Elin Lehrmann[3], Yongqing Zhang[3], Kevin G. Becker[3], Susan M. Freier[6], Yuelin Zhu[7], Sven Diederichs[5,8], Supriya G. Prasanth[1], Ashish Lal[4], Myriam Gorospe[3] and Kannanganattu V. Prasanth[1,*]

[1]Department of Cell and Developmental Biology, University of Illinois at Urbana-Champaign, 601 S Goodwin Avenue, Urbana, IL 61801, USA, [2]Department of Biochemistry and Molecular Biology, Medical University of South Carolina, Charleston, SC 29425, USA, [3]Laboratory of Genetics and Genomics, National Institute of Aging-Intramural Research program, NIH, Baltimore, MD 21224, USA, [4]Regulatory RNAs and Cancer Section, Genetics Branch, Center for Cancer Research, National Cancer Institute, Bethesda, MD, USA, [5]Division of RNA Biology and Cancer, German Cancer Research Center (DKFZ), Im Neuenheimer Feld 280, D-69120 Heidelberg, Germany, [6]Ionis Pharmaceuticals Inc, Carlsbad, CA, USA, [7]Molecular Genetics Section, CCR, NCI, NIH, Bethesda, MD, USA and [8]Division of Cancer Research, Dept. of Thoracic Surgery, Medical Center – University of Freiburg, Faculty of Medicine, University of Freiburg, Breisacher Str. 115, 79106 Freiburg & German Cancer Consortium (DKTK), Freiburg, Germany

Received December 20, 2017; Revised July 12, 2018; Editorial Decision July 19, 2018; Accepted July 23, 2018

ABSTRACT

Long non-coding RNAs (lncRNAs) regulate vital biological processes, including cell proliferation, differentiation and development. A subclass of lncRNAs is synthesized from microRNA (miRNA) host genes (*MIRHGs*) due to pre-miRNA processing, and are categorized as miRNA-host gene lncRNAs (lncmiRHGs). Presently, the cellular function of most lncmiRHGs is not well understood. We demonstrate a miRNA-independent role for a nuclear-enriched lncmiRHG in cell cycle progression. *MIR100HG* produces spliced and stable lncRNAs that display elevated levels during the G1 phase of the cell cycle. Depletion of *MIR100HG*-encoded lncRNAs in human cells results in aberrant cell cycle progression without altering the levels of miRNA encoded within *MIR100HG*. Notably, *MIR100HG* interacts with HuR/ELAVL1 as well as with several HuR-target mRNAs. Further, *MIR100HG*-depleted cells show reduced interaction between HuR and three of its target mRNAs, indicating that *MIR100HG* facilitates interaction between HuR and target mRNAs. Our studies have unearthed novel roles played by a *MIRHG*-encoded lncRNA in regulating RNA binding protein activity, thereby underscoring the importance of determining the function of several hundreds of *lncmiRHGs* that are present in human genome.

INTRODUCTION

Human cells utilize only 2% of their genome to generate transcripts with protein-coding sequences. However, a large portion of the genome is transcribed into noncoding RNAs (ncRNAs) with no apparent protein-coding potential. NcRNAs could be broadly classified into two subclasses. Small non-coding RNAs are transcripts smaller than 200 nucleotides, and some well-known examples of small ncRNAs include microRNAs (miRNAs), small interfering RNAs (siRNAs) and Piwi-interacting RNAs (piRNAs). On the other hand, ncRNAs that are larger than 200 nucleotides are defined as long-noncoding RNAs (lncRNAs) (1). Current estimates indicate that human genome harbors >16,000 lncRNA genes (Human GENCODE Release, version 27: http://www.gencodegenes.org/

*To whom correspondence should be addressed. Tel: +1 217 244 7832; Email: kumarp@illinois.edu
Correspondence may also be addressed to Je-Hyun Yoon. Tel: +1 843 792 8598; Email: yoonje@musc.edu
Correspondence may also be addressed to Vidisha Tripathi. Tel: +91 20 25708242; Email: tvidisha@nccs.res.in
†The authors wish it to be known that, in their opinion, the first two authors should be regarded as joint First Authors.
Present address: Vidisha Tripathi, National Center for Cell Science, Pune, India.

stats/current.html). LncRNA expression is dynamically regulated in a cell-, tissue- or development-specific fashion. Recent studies revealed that lncRNAs play important roles in several biological processes, including cell cycle progression, DNA damage response, stem cell fate determination and X-chromosome inactivation (1–5). In addition, aberrant expression of a large number of lncRNAs is associated with various diseases, including cancer, and a few of the candidate lncRNAs are shown to regulate cancer-related signaling pathways (6–9). At the molecular level, lncRNAs adopt various mechanisms to regulate chromatin organization, gene transcription, and post-transcriptional RNA processing (3). LncRNAs can also serve as molecular scaffolds to modulate nucleic acid-nucleic acid or nucleic acid-protein interactions, or to titrate away proteins and miRNAs from chromatin regions (2,5).

LncRNAs are sub-categorized based on their genomic locations, expression patterns, or functions (10). Some lncRNAs harbor miRNAs within their exonic or intronic sequences, and hence are referred as miRNA-host gene lncRNAs (lnc-miRHGs). miRNAs are short non-coding RNAs (usually 22nt), and they regulate target gene expression post-transcriptionally by promoting mRNA decay or inhibiting translation (11). In the genome, miRNAs are produced from intergenic (28%), intronic (55%), or exonic (17%) regions of host pre-mRNAs or host lncRNAs (12–15). For example, ∼17.5% of miRNAs are produced from lnc-miRHGs (16). The biogenesis and function of miRNAs that are processed from lnc-miRHGs have been well studied. In addition, several lnc-miRHGs show aberrant expression in diseases, hence could serve as important diagnosis or prognosis markers (17–19). However, it is not clear whether the stable and properly spliced pool of lnc-miRHGs, which are processed from the pri-miRHG during miRNA processing plays any vital cellular functions, or merely act as non-functional byproducts of miRNA processing. Very few studies thus far have determined miRNA-independent roles of lnc-miRHGs. For example, *PVT1* oncogenic lncRNA, which is processed from the *MIRHG* harboring miR-1204, miR-1205, miR-1206, miR-1207-5p, miR-1207-3p and miR-1208, positively regulates c-Myc expression and activity (20,21). Similarly, the exon-bearing and completely processed *RMST* lncRNA (contains miR-1251 within its intronic region) and *MIR31HG* (contains miR-31 within its intron) are known to play vital roles in neurogenesis and cancer progression, respectively (22,23). Finally, the H19 lncRNA that is processed from a *MIRHG* plays crucial oncogenic role (19). All of these studies indicate miRNA-independent roles of lnc-miRHGs in various key biological processes.

In the present study, we discovered that multiple lnc-miRHGs, including *MIR100HG*, are differentially expressed during specific stages of the cell cycle. We observed that the levels of *MIR100HG* are elevated during G1 stage, and depletion of *MIR100HG* causes defects in cell cycle progression. More importantly, the spliced, abundant and nuclear-enriched *MIR100HG* exerts its function in a miRNA-independent manner. We demonstrated that *MIR100HG* interacts with RNA-binding-proteins (RBPs), such as HuR and several of HuR-target mRNAs. Mechanistic studies indicate that *MIR100HG* facilitates the interaction between HuR and a subset of its target mRNAs. We conclude that *MIR100HG* potentially serves as a binding platform for both HuR and its target mRNAs, thus modulating HuR-target mRNA interactions.

MATERIALS AND METHODS

Cell culture

U2OS cells were grown in DMEM containing high glucose, supplemented with Penicillin–Streptomycin (Corning) and 10% fetal bovine serum (FBS) (HyClone, GE). WI-38 was grown in MEM containing high glucose, 10% FBS, and 1% non-essential amino acid (NEA). Cell cycle synchronization of U2OS cells was performed as described previously (24).

Plasmid construction

Full-length *MIR100HG* (isoform MIR100HG:9 in lncipedia or NR_024430.1 in NCBI) was amplified from U2OS cDNA and was cloned into PGMT-easy vector (Promega) or pCDNA3. Three *MIR100HG* fragments were sub-cloned from full-length construct into PGMT-easy vector.

Antisense oligonucleotide, 2′MOE and siRNA treatment

Phosphorothioate internucleosidic linkage-modified DNA antisense oligonucleotides (ASOs) were designed and synthesized by Ionis Pharmaceuticals, Inc. They are modified with five 2′-*O*-methoxyethyl nucleotides on the 5′ and 3′ ends and 10 consecutive oligodeoxynucleotides to support RNase H activity. 2′MOE with phosphorothioate backbone was designed and synthesized by Ionis Pharmaceuticals, Inc., for blocking *MIR100HG* interaction with mRNAs. ASOs, MOEs and siRNAs (SigmaGenosys, USA) against *MIR100HG* or HuR were transfected into cells using Lipofectamine RNAiMax (Invitrogen, USA).

cDNA microarray

Total RNA (250 ng) was prepared in triplicate using the RNeasy Mini kit (Qiagen) and labeled using the IlluminaTotalPrep RNA amplification kit (Ambion). Microarrays were performed with the HumanHT-12 v4 Expression BeadChip kit (Illumina). After hybridization, raw data were extracted with Illumina GenomeStudio software, raw probe intensities were converted to expression values using the lumi package in Bioconductor with background correction, variance stabilization and quantile normalization. Differential expression between different conditions was computed by an empirical Bayes analysis of a linear model using the limma package in Bioconductor. Adjusted *P*-values were calculated with the Benjamini and Hochberg method, and differentially expressed genes were selected with adjusted *P*-value ≤ 0.05 and a fold change ≥ 1.50.

RESULTS

MIR100HG-encoded lncRNAs show elevated levels during G1 phase of the cell cycle

In cancer cells several miRNAs display cell cycle-regulated expression, and are modulated by cell cycle-regulated onco-

genic transcription factors including c-Myc (25,26). To determine the involvement of miRNAs and their host genes in cell proliferation, we looked at the expression of several of the c-Myc target *MIRHG*s, including *PVT1*, *MIR17HG* and *MIR100HG* during the cell cycle (Supplementary Figure S1A). These *MIRHG* loci or the encoded miRNAs are involved in cell proliferation or cancer progression (27–33). RT-qPCR analyses using primer pairs from exonic-intronic as well as intronic regions in cell cycle synchronized U2OS (osteosarcoma) (Supplementary Figure S1B) cells revealed elevated levels of *pri-MIR100HG* and *PVT1* transcripts, specifically during G1 phase of the cell cycle (Figure 1Aa and Supplementary Figure S1Ca). Pri-MIR17HG RNA showed elevated levels both in the mitotic and G1 stages of the cell cycle (Supplementary Figure S1Cb). Elevated *PVT1* expression is highly correlated with cell proliferation and tumor formation (21). MIR17-92 miRNA cluster is a known oncomir (34,35), and *MIR100HG*-encoded miRNAs (miR-100, let7a2 and miR-125b1) are known to regulate cell proliferation (27–33). These results indicate that the expression of these lnc-miRHGs is dynamically regulated during the cell cycle.

MiR-100, let7a2 and miR-125b1 are embedded within the last intron of *MIR100HG* (Figure 1B and Supplementary Figure S1Ac, Figure 1B showing isoform MIR100HG:9 in lncipedia or NR_024430.1 in NCBI). It is interesting to note that *MIR100HG*-encoded miRNAs are shown to play pro- as well as anti-proliferative roles. For example, let-7 miRNA family is a known tumor suppresser miRNA, and acts as a negative regulator of cell growth. Both miR-125-b1 and miR-100 act as oncogenic or tumor suppressor miRNAs in various cancers (27–33). Because of this, we were interested in determining whether the exon-bearing lncRNA/s transcribed from *MIR100HG* locus play any role in cell proliferation. *MIR100HG* produces several isoforms of *MIR100HG* lncRNAs (in the rest of the manuscript, we refer *MIR100HG* for exon-bearing lncRNAs from *MIR100HG* locus) due to alternative splicing and differential promoter usage (Supplementary Figure S1Ac). In order to test the relative levels of the spliced *MIR100HG* during the cell cycle, we performed RT-qPCR analyses in RNA samples from synchronized U2OS cells using exon–exon junction primer pairs to amplify the exonic region (exon 2–exon 3 and exon 3–exon 4) shared by most of the *MIR100HG* isoforms. Similar to what we observed in the case of *pri-miR100HG* RNA, even the spliced *MIR100HG* showed elevated levels, specifically during G1 (Figure 1Ab and Ac). Exonic primers targeting the last exon (both spliced and *pri-miR100HG* transcripts) also displayed same expression pattern (Supplementary Figure S1Cc). *MIR100HG* was found to be a predominantly nuclear and relatively stable lncRNA with a half-life of ∼75 min (Figure 1C, Supplementary Figure S1Da). Interestingly, *MIR100HG* stability was regulated during cell cycle, as observed by its enhanced stability during G1 phase over S-phase of the cell cycle (Supplementary Figure S1Db).

Next, we tested the levels of mature and precursor miR-100 and miR-125b1 (both are generated from *MIR100HG* locus) during the cell cycle by using Taqman and cleavage assay (an assay that quantifies the production of pre-miRNA) respectively (36). The levels of mature, pre-miRNA and pri-miRNAs did not change significantly during the cell cycle (Figure 1Da and Db, Supplementary Figure S1E). The absence of much fluctuation of mature miRNAs during the cell cycle could be attributed to their enhanced stability. The dynamic expression and differential stability of the nuclear-restricted *MIR100HG* during the cell cycle implies that the lncRNAs produced from the *MIR100HG* locus might participate in cell cycle progression.

Elevated levels of *MIR100HG* were previously observed in megakaryoblastic leukemia (AMKL) cell lines, and high levels of *MIR100HG* were correlated with poor prognosis in cases of cervical cancer patients (37,38). We therefore determined the levels of *MIR100HG* in various cancer cell lines and in non-tumorigenic cells. We compared the level of *MIR100HG* among human diploid lung fibroblast (WI-38), cervical cancer (HeLa), bone osteosarcoma (U2OS) and highly tumorigenic and metastatic MCF10CA1a.cl1 breast cancer (M4) cell lines (39,40). Compared to the three cancer cell lines, non-tumorigenic diploid WI-38 cells showed lower levels of *MIR100HG* (Supplementary Figure S1Fa). In addition, we also determined the levels of *MIR100HG* in a MCF10A-derived isogenic breast cancer progression cell line model system, represented by M1-M4 cell lines. M1 represents non-tumorigenic MCF10A cells, and M2 represents HRAS-expressing M1 cells but show very low tumorigenic potential when implanted in immune compromised mice. M3 and M4 were isolated from tumor samples from mice that were xenografted with M2 cells. M3 cells are highly tumorigenic and form well-differentiated tumors in mice, but they display low metastatic potential. On the other hand, M4 cells form highly undifferentiated tumors and very efficiently metastasize in the lungs (39–43). We observed that *MIR100HG* levels were dramatically increased in both M3 and M4 cells compared to M1 and M2 cells (Supplementary Figure S1Fb). These results suggest that G1-phase upregulated *MIR100HG* tends to show elevated expression in cancer cells. Publicly available RNA-seq data sets from U2OS cells showed expression of *MIR100HG* (Supplementary Figure S1G). Further, RNA copy number analyses revealed that asynchronous U2OS and M4 cells contained ∼68 and ∼365 copies of processed *MIR100HG* lncRNAs respectively (Supplementary Figure S1H). Northern blot (NB) using a probe from exon 4 of *MIR100HG* showed a specific signal of ∼3.5 kb (Figure 1Ea). NB using a probe comprising of exons 1–3 showed two discrete bands, one at 3.5 kb and another weak band at 5 kb (Figure 1Eb), indicating that *MIR100HG* produces multiple isoforms of *MIR100HG* via alternative splicing (please also see supplementary Figure S1Ac). Finally, we determined the protein-coding potential of *MIR100HG* isoforms utilizing the integrated database of annotated human lncRNAs: Lncipedia.org (https://lncipedia.org/), and identified *MIR100HG* as a non-coding transcript (Supplementary Figure S1I). In summary, we identified a stable, abundant, spliced, G1 phase-enriched, and nuclear restricted lncRNA, transcribed from the *MIG100HG* locus that showed elevated expression in several of the tested cancer cell lines.

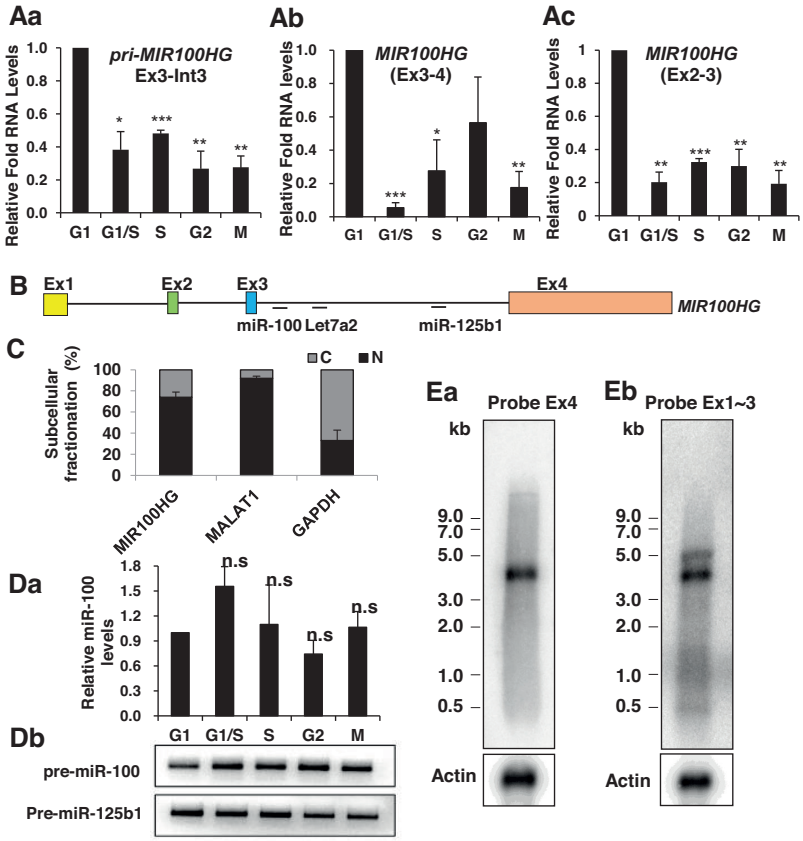

Figure 1. *MIR100HG* shows elevated levels during G1 phase of cell cycle. (**A**) RT-qPCR analyses to determine the relative abundance of *pri-MIR100HG* (a) and spliced *MIR100HG* (b) during the cell cycle. Primers in (a) target the exon 3-intron 3 junction, (b) target the exons 3–4 junction, and in (c) exons 2–3 junction. (**B**) Schematic of *MIR100HG* gene. Positions of miR-100, let7a2, and miR-125b1 are indicated using horizontal lines. *MIR100HG* isoform in the schematic is MIR100HG:9 in lncipedia or NR_024430.1 in NCBI. (**C**) RT-qPCR analysis to determine the relative abundance of *MIR100HG* in the nuclear (N) or cytoplasmic (C) fraction. MALAT1 and GAPDH RNA were used as control RNAs for nuclear and cytoplasmic fractions respectively. (**D**) Taqman RT-qPCR assay (a) and RNA cleavage assay (b) to reveal the relative abundance of mature and pre-miR-100 during cell cycle in U2OS cells. (**E**) Northern blot analyses to identify *MIR100HG* transcript isoforms. Probes spanning exon 4 (a) and exons 1–3 (b) were used respectively. ACTB (beta-Actin) was used as loading control. $*P \leq 0.05$, $**P \leq 0.01$, $***P \leq 0.001$, $****P \leq 0.0001$ by two-tailed Student's *t*-test, $n = 3$. Error bars represent standard deviation from three biological replicates.

MIR100HG regulates cell cycle progression

To determine the involvement of *MIR100HG* during the cell cycle, we successfully depleted *MIR100HG* by transfecting U2OS cells with modified DNA antisense oligonucleotides (ASO1 and ASO2) (Figure 2A and Supplementary Figure S2A) for 48 h. *MIR100HG*-depleted cells did not show any significant change in the total cellular levels of miR-100, pre and pri-miR-100, and pre-miR-125b1 post 48 h of ASO transfection (Figure 2B, Supplementary Figure S2B). In addition, we examined the RNA levels of several known miR-100 target mRNAs in control and *MIR100HG*-depleted cells (31,44–47). RT-qPCR and immunoblot analyses results revealed that both control and *MIR100HG*-depleted cells showed comparable levels of several of the tested miR-100 target mRNAs (Figure 2C and Supplementary Figure S2C). These results confirm that cells depleted of *MIR100HG* for 48 h did not show changes in either the levels or activity of the *MIR100HG* intron-encoded miRNAs. It is possible that miR-100 and miR-125b1 are stable miRNAs, therefore the depletion of *MIR100HG* for 48 h did not affect the steady-state levels of these miRNAs. Alternatively, *MIR100HG* gene locus could produce different sets of transcripts, some of which will be processed to synthesize exon-bearing lncRNAs, and the others act as the microRNA host transcripts.

To determine the involvement of *MIR100HG* in cell proliferation, we performed flow cytometry analysis and found that *MIR100HG*-depleted U2OS cells showed elevated levels of G2/M population with a concomitant reduction in G1 population (ASO1 and ASO2, Figure 2D). In addition, depletion of *MIR100HG* in U2OS cells using a third ASO from exon 2 (ASO3; Supplementary Figure S2A) also showed a similar phenotype (Supplementary Figures S2D and S2E). We also depleted *MIR100HG* using an independent siRNA targeting exon 4 (Supplementary Figures S2A and S2F). Cells depleted of *MIR100HG* using siRNA also showed G2/M arrest without affecting the mature miR-100 levels, confirming the specificity of the cell cycle phenotype (Supplementary Figures S2G and S2H). Finally, we performed rescue experiments by overexpressing the full-length spliced *MIR100HG* isoform in cells depleted of the endogenous *MIR100HG*. We observed that the *MIR100HG* cDNA could partially rescue the G2/M arrest phenotype

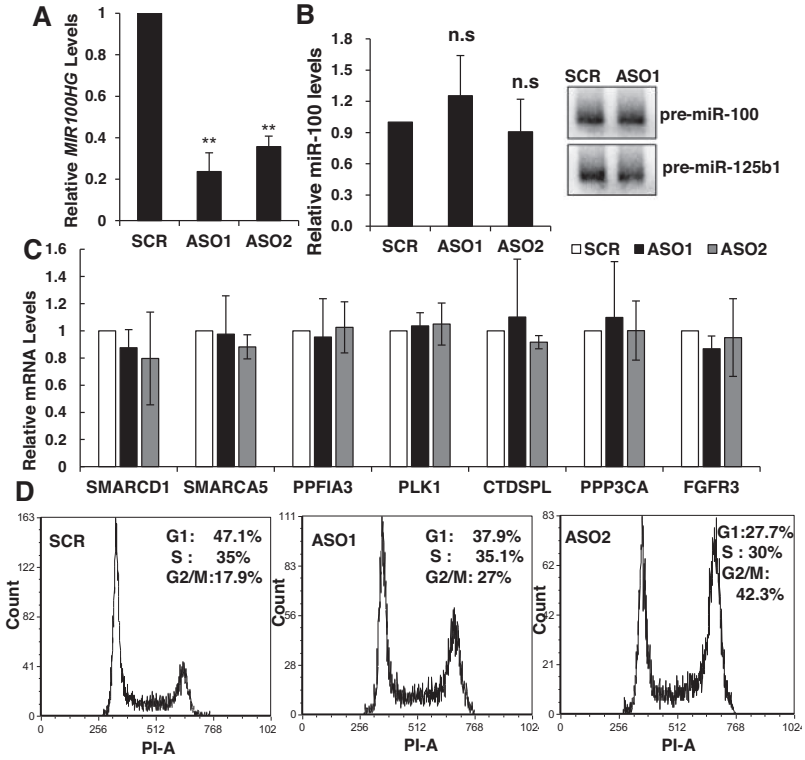

Figure 2. *MIR100HG* depletion results in cell cycle arrest. (**A**) RT-qPCR to determine the relative levels of *MIR100HG* in U2OS cells transfected with control (SCR) or antisense oligonucleotides targeting *MIR100HG* (ASO1, ASO2). (**B**) Taqman RT-qPCR assay to reveal relative levels of miR-100 in control (SCR) and *MIR100HG*-depleted (ASO1 and ASO2) cells. Right: RNA cleavage assay to determine the levels of pre-miR-100 and pre-miR-125b1 in control and *MIR100HG*-depleted cells. (**C**) RT-qPCR to determine the relative levels of several miR-100 target gene mRNAs in control (SCR) and *MIR100HG*-depleted (ASO1 and ASO2) cells. (**D**) Flow cytometry analyses in control (SCR) and *MIR100HG*-depleted (ASO1 and ASO2) U2OS cells. Quantification was performed using FCS Express. $*P \leq 0.05$, $**P \leq 0.01$, $***P \leq 0.001$, $****P \leq 0.0001$ by two-tailed Student's *t*-test, $n = 3$. Error bars represent standard deviation.

(Supplementary Figure S2I). This data confirmed the specificity of the knockdown phenotype, and further indicated microRNA-independent cell cycle role for lncRNAs processed from the *MIR100HG* locus.

In addition to G2/M arrest, *MIR100HG* depletion in diploid fibroblasts (WI-38) also resulted in defective S phase progression, as observed by reduced bromo-deoxy uridine (BrdU) uptake in the BrdU/propidium iodide (PI) flow cytometry analysis (Supplementary Figure S2J). In order to determine the rate at which cells progress through S phase, we synchronized control and *MIR100HG*-depleted cells in G1/S using aphidicolin, and released them into S phase for the indicated time points (4, 8 and 12 h post-aphidicolin release). We found that, when compared to control ASO-treated cells, *MIR100HG*-depleted cells displayed a delay in their progression through S phase (Supplementary Figure S2K). This was obvious in the 8 h release time point in which the control cells had progressed into G2/M phase, but a fraction of *MIR100HG*-depleted cells continued to have DNA content between 2C and 4C (observed by the broader peak), implying the slow S-phase progression. Similarly, a proportion of control cells progressed into G1 phase at the 12 h release time point. However, most of the *MIR100HG*-depleted cells at the 12 h time point accumulated in G2/M phase and failed to enter G1 phase.

In order to gain insight into the gene expression program that is affected in *MIR100HG*-depleted cells, we performed transcriptome microarray in control and *MIR100HG*-depleted U2OS cells. We identified 722 downregulated genes ($\leq$0.67 fold) and another 577 upregulated genes ($\geq$1.5-fold) in *MIR100HG*-depleted cells. Pathway analyses revealed that these genes, whose expression levels are altered in *MIR100HG*-depleted cells, play vital roles in crucial pathways controlling cell growth, including cell cycle, cell proliferation, cell death and survival, further supporting the cellular phenotype observed in *MIR100HG*-depleted cells (Supplementary Table S1, Supplementary Figure S2L).

In summary, we found that human diploid and cancer cells depleted of *MIR100HG* showed defects in cell cycle progression, as observed by slow S phase progression and/or G2/M arrest. We propose that that G1-upregulated *MIR100HG* might play a crucial role in the entry of cells into G1 phase of the cell cycle, and its depletion results in defects in G1 entry, resulting in cells being arrested in G2/M phase of the cell cycle.

MIR100HG interacts with HuR and influences the association of HuR with its target mRNAs

It is known that several nuclear-retained lncRNAs regulate gene expression by influencing the localization and/or ac-

tivity of various RBPs (5,48–50). In order to gain mechanistic insights into the role of *MIR100HG*, we performed RNA-affinity pull-down in U2OS nuclear extracts using biotin-labeled *MIR100HG* followed by mass-spectrometry (Figure 3A). Mass spectrometry showed potential interaction between *MIR100HG* and several RNA binding proteins (RBPs) (Supplementary Figure S3A). Further, we validated the interaction between *MIR100HG* and RBPs such as HuR, PTB and PUF60, by biotin–RNA pull-down followed by immunoblotting using nuclear extracts (Figure 3B). HuR, PTB, PUF60, but not AUF1, showed positive interaction with *MIR100HG*.

HuR is a ubiquitous member of neuronal ELAV-like proteins. It recognizes AU-rich elements (ARE) or U-rich sequences, typically within the 3′-untranslated region (UTR) of RNAs (51–53). HuR is known to control multiple biological events including the cell cycle, apoptosis, and cancer progression (54–58). We therefore investigated the functional significance of the interaction between HuR and *MIR100HG*. We first confirmed the interaction between HuR and endogenous *MIR100HG* by HuR ribonucleoprotein (RNP) immunoprecipitation (RIP) analysis in cell cycle synchronized cell extracts followed by RT-qPCR. HuR showed enhanced interaction with *MIR100HG* during the G1/S phase of the cell cycle (Figure 3C). Immunoblotting in cell cycle synchronized cell extracts indicated that the level of HuR in G1/S was comparable to most other cell cycle stages except G1 phase, where the levels were found to be relatively low (Supplementary Figure S3B). In order to map the sequence elements within *MIR100HG* that interact with HuR, we performed biotin–RNA pull-down followed by Immunoblotting using 3 partially overlapping fragments of *MIR100HG* (Figure 3D). We observed that both fragments 2 and 3 within *MIR100HG* interacted with HuR (Figure 3E). Both the HuR-interacting fragments were from the 3′end of the last exon (exon 4) of *MIR100HG*. On the other hand, another RBP SRSF1 failed to interact with any of the fragments, confirming the specificity of HuR: *MIR100HG* interaction (Figure 3E). Interestingly, we found that fragments 2 and 3 contain two U-rich repeats (18 and 15 nt long U-rich repeats respectively, Figure 3D). Based on these data, we conclude that HuR preferentially interacts with the last exon of *MIR100HG*.

HuR is known to regulate the stability or translation of many mRNAs (51,53). To determine whether *MIR100HG* influences the association of HuR with its target mRNAs, we performed HuR RIP followed by microarray using RNA from control and *MIR100HG*-depleted U2OS cells (Supplementary Figure S4A). Interestingly, knockdown of *MIR100HG* significantly decreased the association of HuR with several of its target mRNAs (Supplementary Figures S4B and S4Ca, Supplementary Table S2). Further, by performing HuR-RIP followed by RT-qPCR in control and *MIR100HG*-depleted cells, we confirmed the reduced association of HuR with several of its target mRNAs (MSH3, CCR6, and CCND2; Figure 4A). At the same time, *MIR100HG* depletion did not alter the association of HuR to several constitutively expressed housekeeping gene mRNAs (Supplementary Figure S4Cb). Our results imply that *MIR100HG* positively regulates HuR association with several of its target mRNAs.

It is possible that the aberrant association of HuR to its target mRNAs in *MIR100HG*-depleted cells could be due to reduced levels of these mRNAs. To test this, we checked the steady-state levels of HuR target mRNAs in control and *MIR100HG*-depleted cells using our microarray data set. Depletion of *MIR100HG* did not affect steady-state levels of known HuR target mRNAs (Supplementary Table S1). Microarray results were further validated by RT-qPCR analyses (Figure 4B). We also found that knockdown of *MIR100HG* did not alter either the total levels or the subcellular distribution of HuR (Supplementary Figures S4D and S4E). These findings indicated that the reduction of HuR's association with a subset of its target mRNAs detected upon *MIR100HG* depletion was not due to changes in total levels or localization of HuR, but due to changes in its ability to interact with specific mRNA targets.

It is interesting to note that the strongest interaction between *MIR100HG* and HuR was observed at the G1/S-boundary (Figure 3C). *MIR100HG* level was also relatively low during the G1/S transition (Figure 1A). Although HuR is known to stabilize mRNAs in many instances, recent studies from several laboratories, including ours, have shown that HuR can also destabilize mRNAs and lncRNAs (59–61). In order to determine whether HuR influences the levels of *MIR100HG*, we compared the levels of *MIR100HG* in control and HuR-depleted cells. HuR-depleted cells showed a small but significant increase in the levels of *MIR100HG*, indicating that the association of HuR with *MIR100HG* at the end of G1 phase could also facilitate the destabilization of lncRNA (Figure 4C).

HuR participates in several crucial post-transcriptional processes such as mRNA stability, and is also known to regulate translation (62). We tested whether *MIR100HG*- or HuR-depleted cells showed any change in the mRNA stability or protein levels of a few HuR targets. Both *MIR100HG* and HuR-depleted cells did not show any change in the stability of the tested mRNAs (Supplementary Figures S4F and S4G). Interestingly, *MIR100HG*- or HuR-depleted cells showed decrease in the protein levels of CCND2/Cyclin D2, a known HuR target (Figure 4Da and Db, Supplementary Figure S4H). Furthermore, we rescued the levels of CCND2 in *MIR100HG*-depleted cells by exogenously expressing one of the *MIR100HG* isoforms (Figures 1B and 4E). *MIR100HG* seems to regulate the cellular levels of CCND2 protein. It is possible that reduced interaction between HuR and CCND2 mRNA observed in *MIR100HG*-depleted cells contributes to reduced levels of CCND2 protein.

U-rich domains within *MIR100HG* modulate the interaction between *MIR100HG* and HuR RNP complex

Next, we probed into the potential mechanism utilized by *MIR100HG* to influence the interactions between HuR and its target mRNAs. LncRNAs is known to function as scaffold to stabilize RNA: protein, DNA: protein, and protein: protein interactions (2). We determined whether *MIR100HG*, by interacting with both HuR and its target mRNAs, modulates HuR-target mRNA association or stabilizes HuR-target mRNA RNP complex assembly. To test this, we used computational prediction tools (63)

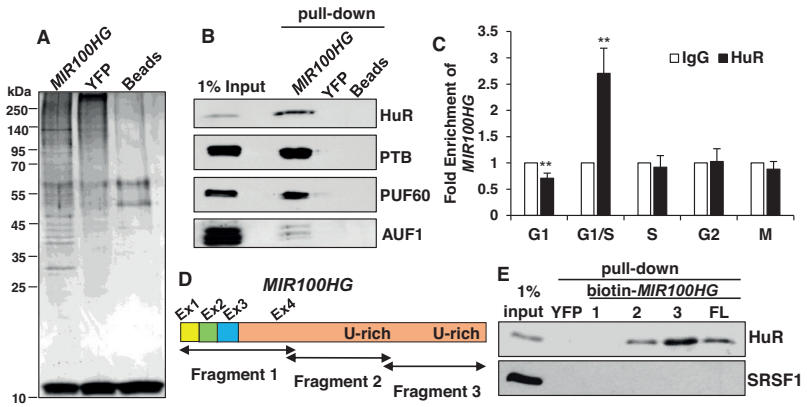

Figure 3. *MIR100HG* interacts with RNA binding protein HuR. (**A**) Representative silver-stained SDS-PAGE gel showing specific bands of the extracts incubated with biotin-labeled *MIR100HG* followed by RNA pull-down assay. Nuclear extract of U2OS was used in biotin–RNA pulldown assay. RNA Pull-down using biotin-labeled YFP RNA (lane 2, YFP) or beads only without RNA (lane 3, Beads) served as controls. (**B**) *MIR100HG*-interacting proteins identified by mass spectrometry analyses were validated by *in vitro* biotin–RNA pull-down followed by immunoblotting. RNA Pull-down was performed using biotin-labeled full-length *MIR100HG*. YFP and beads serve as control. (**C**) HuR-RIP or IgG-RIP followed by RT-qPCR during specific stages of cell cycle (G1, G1/S, S, G2, M phases) to determine the interaction between HuR and *MIR100HG*. RT-qPCR data was normalized over GAPDH mRNA. (**D**) Schematic showing three fragments of *MIR100HG*. (**E**) *In vitro* biotin–RNA pull-down followed by immunoblotting to detect the interaction between HuR and specific fragments (1, 2 and 3) or full length (FL) *MIR100HG*. YFP RNA was used as negative control. SRSF1 served as a negative control. $*P \leq 0.05$, $**P \leq 0.01$, $***P \leq 0.001$, $****P \leq 0.0001$ by two-tailed Student's *t*-test, $n = 3$. Error bars represent standard deviation.

to find mRNAs that have sequence complementarity with *MIR100HG*. From the prediction analysis, we narrowed down the candidate mRNAs containing at least 18nt of sequence complementarity with *MIR100HG* with >88% identity. From the prediction, we found that 7706 mRNAs met these criteria (Supplementary Table S3), while only 24 of them were identified as HuR-interacting mRNAs by our HuR RIP analysis (Supplementary Table S3). Our results suggested that HuR and *MIR100HG* could bind to several shared target mRNAs. Interestingly, most predicted interactions between mRNAs and *MIR100HG* occurred through the first U-rich repeat sequences that present in the last exon of *MIR100HG* (Figure 5A). The low sequence complexity of 18-nt U-repeat indicated low specificity. However, due to the fact that *MIR100HG* interacted with HuR, we asked if *MIR100HG* displayed higher binding affinity to HuR target mRNAs among all of these predicted mRNAs. To test this possibility experimentally, we incubated biotin-labeled *MIR100HG* or YFP mRNA (as a negative control) in total cellular extracts, and performed *in vitro* pull-down followed by RT-qPCR to identify RNAs that interact with *MIR100HG*. We observed significant interaction between *MIR100HG* and either MSH3, CCR6, or CCND2 mRNAs, compared to biotin-labeled YFP RNA. (Figure 5B, *MIR100HG*+MOE-SCR). These three mRNAs were previously shown to interact with HuR in a *MIR100HG*-dependent manner (Figure 4A). Absence of specific association between *MIR100HG* and GPI mRNA confirmed the specificity of the interaction (Supplementary Figure S5A).

We next asked if the U-repeat region within the *MIR100HG* is essential for facilitating the lncRNA: mRNA interactions. To answer this question, we designed a 20 nt-long 2′-*O*-methoxyethyl antisense oligos (MOE; MOE-100), which is complementary to the U-rich repeat region within the *MIR100HG* (Figure 5A). For the assay, we pre-incubated biotin-*MIR100HG* with either control or this A-rich MOE (MOE-100); then incubated the RNA with cellular extract, and finally determined the efficiency with which *MIR100HG* interacted with MSH3, CCR6, CCND2 or GPI mRNAs. Pre-incubation of biotin-labeled *MIR100HG* with MOE, which hybridized to U-rich sequences within the lncRNA, completely abolished the interaction between *MIR100HG* and either MSH3, CCR6 or CCND2 mRNAs (Figure 5B and Supplementary Figure S5A, *MIR100HG*+MOE-100). These results reveal that the U-rich sequences that present in the 3′ end of *MIR100HG* promotes its interaction with specific members of HuR-target mRNAs.

We also determined whether the U-rich sequence element also facilitates the interaction between *MIR100HG* and HuR. For this, we performed RNA-affinity pull-down in cell extracts using biotin-labeled *MIR100HG* which was pre-incubated with biotin-labeled control (SCR) or A-rich MOE (MOE-100) oligos followed by immunoblotting. HuR showed strong interaction with *MIR100HG* only in SCR-MOE pre-incubated extracts and not in A-rich MOE-pre-incubated extracts (Figure 5C), indicating that *MIR100HG* utilizes the U-rich motif to interact with both HuR and HuR-target mRNAs. Finally, we were interested to see the involvement of *MIR100HG* U-rich sequence element in the in vivo interaction between HuR and its target mRNAs. Towards this, we performed HuR RIP followed by RT-qPCR in cells transfected with control and A-rich MOE-oligos to determine the interaction between HuR and its target mRNAs. We found that the A-rich MOE (MOE-100), which could disrupt the interaction between *MIR100HG* and HuR and HuR target mRNAs, also attenuated the interaction between HuR and its target mRNAs, including MSH3 and CCND2 (Figure 5D). Finally, we also found that the protein levels of CCND2 and MSH3 were reduced in cells transfected with the A-rich MOE-oligos. (Figure 5E, Supplementary Figure S5B). These results suggest that the U-rich sequences within *MIR100HG* are the necessary for *MIR100HG*'s regulatory role in HuR activ-

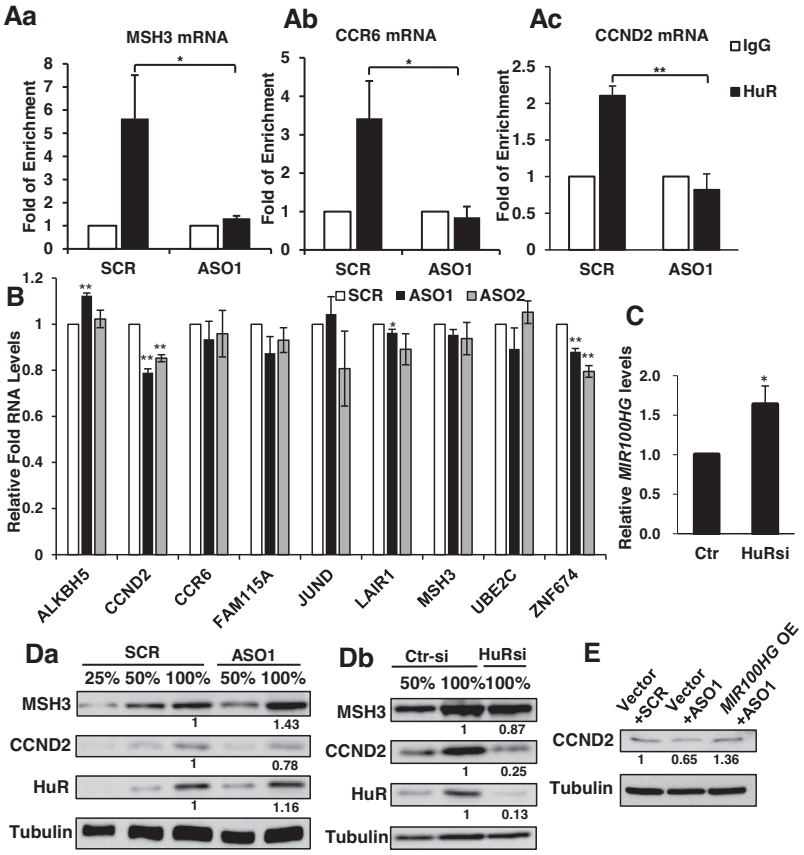

Figure 4. *MIR100HG* regulates the interaction between HuR and its target mRNAs. (**A**) HuR RIP followed by RT-qPCR in control (SCR) and *MIR100HG*-depleted (ASO1) cells to determine the interaction between HuR and targets, including (a) MSH3 mRNA, (b) CCR6 mRNA and (c) CCND2 mRNA. RT-qPCR data was normalized to GAPDH mRNA. (**B**) RT-qPCR to determine the relative levels of several of the HuR-target mRNAs in control (SCR) and *MIR100HG*-depleted (ASO1 & ASO2) U2OS cells. (**C**) RT-qPCR to determine the relative levels of *MIR100HG* in control and HuR-depleted cells. (**D**) Immunoblot to detect the relative levels of HuR and protein levels of its target mRNAs in control (SCR) and *MIR100HG*-depleted (ASO1) cells (a), and in control (Ctr-si) and HuR-depleted (HuRsi) cells (b). α-Tubulin was included as loading control. The relative protein amount in knockdown samples (with 100% loading) was normalized relative to α-Tubulin, and compared to control. Quantification was performed using ImageJ, quantification results for three repeats is shown in Supplementary Figure S4H. (**E**) Immunoblot to detect the relative protein level of CCND2 in U2OS cells transfected with empty vector or *MIR100HG* overexpression vector (same plasmid as in Supplementary Figure S2I), with control or *MIR100HG* antisense oligo (ASO1). Quantification was performed using ImageJ. α-Tubulin was included as loading control. $*P \leq 0.05$, $**P \leq 0.01$, $***P \leq 0.001$, $****P \leq 0.0001$ by two-tailed student's *t*-test. For (Aa-b, B, E), $n = 3$. For (Ac), $n = 2$. Error bars represent standard deviation.

ity modulation. Our results reveal that the interaction between *MIR100HG* and HuR or its target mRNAs modulates HuR-association to its target mRNAs.

DISCUSSION

Human lncRNAs play crucial roles in several cellular processes such as cell proliferation and differentiation. Most lnc-miRHG studies have focused on understanding the mechanisms whereby cells synthesize miRNAs from their host transcripts. Very few studies thus far have looked at the potential miRNA-independent roles and the mechanism of action of lncRNAs that are processed from the exonic regions of *MIRHG* primary transcripts. In the present study, we provided evidence for the miRNA-independent role for a lnc-miRHG. We found *MIR100HG* levels to be elevated during G1 phase of the cell cycle, and cells depleted of *MIR100HG* showed defects in their entry into G1, supporting *MIR100HG*'s role in cell cycle progression. Furthermore, mechanistic studies revealed that *MIR100HG* acts as a scaffold to modulate the interaction between HuR and its target mRNAs.

It is generally believed that the role of *MIRHG* is to produce miRNAs, and the lncRNAs that are processed from *MIRHG* primary transcripts do not execute any significant role. However, few recent studies have reported miRNA-independent roles played by lnc-miRHGs. (20,22–23,36). These studies underscore the functional significance of this class of lncRNAs, which is ignored before, and indicate the importance of understanding the independent roles played by *MIRHG*-encoded lncRNAs. Our study demonstrates the involvement of *MIR100HG* in the cell cycle and its role in regulating the affinity of an RBP to its target mRNAs, which further underscores the importance of determining the role of several hundreds of lnc-miRHGs in human genome.

RNA pull-down followed by mass spectrometry analyses revealed that *MIR100HG* interacts with several RBPs, including HuR, PTB and PUF60. HuR is a ubiquitously expressed member of the Hu/ELAV family of proteins. It

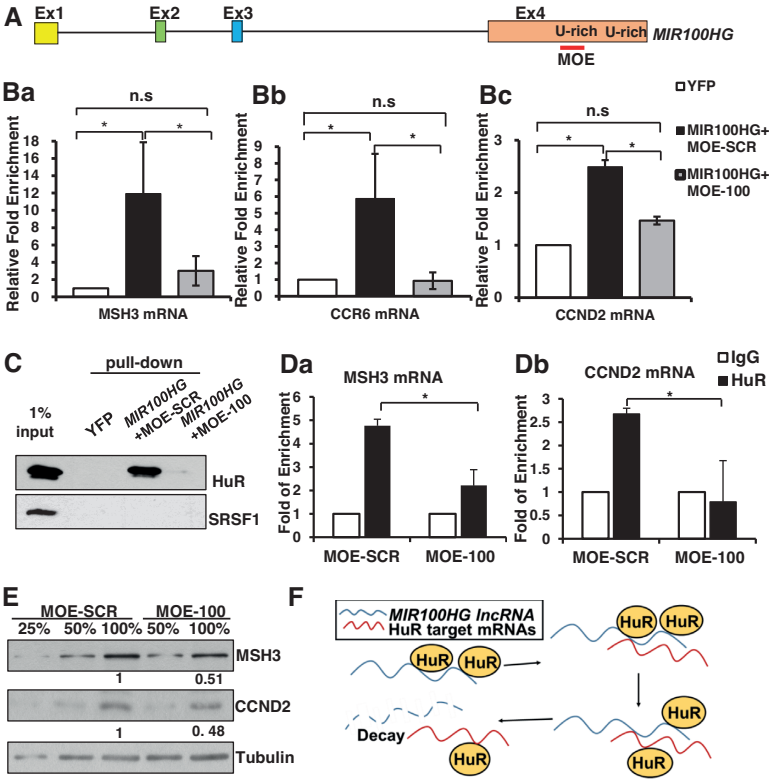

Figure 5. U-rich domains within *MIR100HG* facilitates the interaction between *MIR100HG* and HuR or HuR-target mRNAs. (**A**) Schematic showing the position of two U-rich regions and the 2′-*O*-methoxyethyl antisense oligonucleotide (MOE, A-rich) within the last exon of *MIR100HG*. (**B**) *In vitro* biotin–RNA pull-down followed by RT-qPCR to determine the interaction between *MIR100HG* and HuR-target mRNAs in SCR and U-rich targeting MOE-treated extracts. RT-qPCR data was normalized to GAPDH mRNA. Relative fold enrichment of (a) MSH3 mRNA, (b) CCR6 mRNA, and (c) CCND2 mRNA were calculated by comparing over biotin-YFP, which was used as negative control. A non-*MIR100HG*-interacting example GPI mRNA is shown in Supplementary Figure S5A. (**C**) *In vitro* biotin–RNA pull-down followed by immunoblotting to detect the association between *MIR100HG* and HuR in control (MOE-SCR) and *MIR100HG* targeting (MOE-100) MOE pre-incubated samples. YFP RNA was used as negative control. SRSF1 served as a negative protein control. biotin–RNA was pre-incubated with 2′-MOE oligos (MOE-SCR & MOE-100) prior to *in vitro* pull-down. (**D**) HuR RIP followed by RT-qPCR in in SCR and U-rich targeting MOE (MOE-100) treated cells to determine the interaction between HuR and targets, including (a) MSH3 mRNA and (b) CCND2 mRNA. RT-qPCR data was normalized to GAPDH mRNA. Fold of enrichment (relative to IgG) is plotted. (**E**) Immunoblot to detect the protein levels of HuR target genes in control (SCR) and MOE-100 transfected cells. α-Tubulin was used as loading control. The relative fold of protein amount in MOE-100-treated samples (with 100% loading) was normalized over α-Tubulin, and compared to MOE-SCR. Quantification was performed using Image J and quantification results for three repeats is presented in Supplementary Figure S5B. (**F**) Model depicting the potential mode of action of *MIR100HG*. *MIR100HG* lncRNA interacts with both HuR and HuR target mRNAs and increases their local concentration, and thus facilitating HuR-target mRNA interactions. $*P \leq 0.05$, $**P \leq 0.01$, $***P \leq 0.001$, $****P \leq 0.0001$ by two-tailed Student's *t*-test, $n = 4$ for 5B, $n = 3$ for all other figures. Error bars represent standard deviation.

was initially described as an adaptor protein that influences mRNA export (64). High-throughput protein-RNA interaction studies identified several hundreds of RNAs that interact with HuR (52,53). HuR is found to regulate several vital processes such as mRNA stability, translation, and miRNA biogenesis (62,64–65). Besides *MIR100HG*, HuR is shown to interact with several other lncRNAs, including lincRNA-p21, UFC1, OIP5-AS1 and linc-MD1, and influence their activity (36,61,66–67). For example, HuR binding to linc-MD1 prevents Drosha-mediated cleavage and production of pre-miRNA from the linc-MD1 transcript (36). The 3′ end of *MIR100HG* contains two independent U-rich sequence elements, and our *in vitro* pull-down assays demonstrated that HuR interacts with the U-rich sequence elements. Interestingly, *MIR100HG* also utilizes the same U-rich sequence elements to interact with several tested HuR target mRNAs. It is possible that *MIR100HG* could simultaneously interact with both HuR as well as its target mRNA through the U-rich elements. By this, *MIR100HG* bring both HuR and its target mRNA in close proximity, and this can further increase HuR and target mRNA interactions. The reduced interaction between HuR with target mRNAs in *MIR100HG*-depleted cells further strengthens our hypothesis.

Lnc-miRHGs are generally very unstable in nature (16), which indicates that these lncRNAs are degraded rapidly after generating miRNAs, and thus they might not serve other functions. On the other hand, *MIR100HG* was found to be an abundant and stable lncRNA. RNA stability assays revealed that *MIR100HG* showed enhanced stability during G1 phase of the cell cycle. Interestingly, *MIR100HG* showed increased association with HuR during the time window that also coincides with its decreased stability. Furthermore, HuR-depleted cells showed an increase in the level of

MIR100HG, indicating that HuR destabilizes *MIR100HG*. In support of this argument, recent studies from several laboratories, including ours, have provided evidence demonstrating the role of HuR as an RNA-destabilizing factor (60–61,68–70). For example, HuR is known to promote the degradation of lincRNA-p21 by facilitating the recruitment of let-7b/AGO2 complex to the lncRNA (61).

Loss-of-function studies indicate that *MIR100HG* is required for cell cycle progression. Our results are consistent with a previous study, which reported that *MIR100HG* positively regulates cell proliferation in leukemia cells (37). Interestingly, we observed that the levels of only the *MIR100HG*, and not the intron-embedded miRNAs (miR-100 and miR-125b1), were elevated during G1 phase of the cell cycle. Since depletion of *MIR100HG* did not alter the levels of either the *MIRHG*-encoded miRNAs or the mRNAs that are targets of these miRNAs, we concluded that *lncRNA MIR100HG* plays a miRNA-independent role in regulating cell cycle progression. In addition, *MIR100HG* rescue experiments reveal that the spliced *MIR100HG* lncRNA plays a crucial role in cell cycle progression. The *MIR100HG* gene locus synthesizes multiple *MIR100HG* lncRNA transcripts by utilizing multiple promoters. It is possible that only a subset of the isoforms is processed to produce microRNAs whereas rest of them essentially function as host gene of the spliced lncRNAs. Presently, it is not clear how *MIR100HG* regulates cell cycle progression. One possibility could be that *MIR100HG* promotes the interaction between HuR and mRNAs of cell cycle genes. Such association is crucial for the proper functioning of those mRNAs. HuR is known to regulate cell division and checkpoint response through multiple mechanisms, including modulating the stability and translation of key cell cycle regulators, such as cyclins (58). The localization of HuR is also regulated during the cell cycle (71,72), and such dynamic cellular distribution could influence its interaction with target mRNAs as well as other lncRNAs such as *MIR100HG*. To test the involvement of *MIR100HG* in modulating HuR activity, we determined the mRNA stability and protein levels of HuR targets such as MSH3 and CCND2 mRNAs in cells depleted of *MIR100HG*. HuR-depleted cells were used as controls in these experiments. To our surprise, we did not see any significant change in the stability of both these transcripts in cells depleted of either *MIR100HG* or HuR, indicating that HuR does not seem to regulate the stability of these mRNAs. Immunoblot analyses revealed a consistent decrease in the levels of CCND2, and not MSH3 protein, in *MIR100HG* or HuR-depleted cells. This suggests that *MIR100HG* does not modulate the outcome of all of the HuR-target mRNAs in the similar fashion.

Since HuR interacts with several hundred mRNAs (52), and *MIR100HG*-depleted cells showed defects in the association between HuR and a large number of its targets, it would be challenging to identify a single specific target mRNA whose aberrant function contributes to the observed cell cycle arrest upon *MIR100HG* depletion. Alternatively, *MIR100HG* regulates the cell cycle via modulating the activity of other RBPs, and future efforts will be made to test this possibility. In summary, we demonstrated that *MIR100HG* regulates cell cycle progression. Furthermore, we observed that *MIR100HG* interacted with HuR and its target mRNAs in a cell cycle-regulated manner. The U-rich regions within the *MIR100HG* were found to be essential for its interaction with HuR as well as with HuR target mRNAs. Based on this, we propose a model (Figure 5F), whereby the abundant *MIR100HG* interacts with both HuR and its target mRNAs through its U-rich domains. Such interaction further facilitates the association between HuR and its target mRNAs. By this mechanism, *MIR100HG* acts as a 'nucleating site' or 'scaffold' to increase the local concentration of HuR and its target mRNA, thus facilitating HuR target mRNA interactions. In summary, our studies have unearthed novel roles played by a *MIRHG*-encoded lncRNA in regulating RBP activity, thereby underscoring the importance of determining the function of several hundreds of lnc-miRHGs that are present in the human genome.

DATA AVAILABILITY

Sequence data of both cDNA microarray and HUR-RIP microarray have been submitted to NCBI Gene Expression Omnibus (GEO) (http://www.ncbi.nlm.nih.gov/geo/). The accession numbers are: GSE108280 (cDNA microarray) and GSE107836 (HuR RIP).

SUPPLEMENTARY DATA

Supplementary Data are available at NAR Online.

ACKNOWLEDGEMENTS

We would like to thank K.V. Prasanth and S.G. Prasanth lab members for their comments and suggestions. We thank Drs Eric Bolton (UIUC) and M. Hastings (Rosalind Franklin University) for sharing reagents, and Dr P. Yao for mass spectrometry analyses. We thank J. Roy and S. Sudhakar for proof reading the manuscript.

FUNDING

National Institute of Health [1RO1GM088252 to K.V.P., 1RO1GM099669 to S.G.P.]; American Cancer Society [RSG-11-174-01-RMC to K.V.P.]; National Science Foundation [career, 1243372 to S.G.P. and EAGER 1723008 to K.V.P.]; National Institute on Aging intramural Research Program, NIH [Z01-AG000511 to M.G.]; Medical University of South Carolina and Hollings Cancer Center (to J.H.Y.); National Institute on Cancer Intramural Research Program, NIH (to A.L.). The funders had no role in study design, data collection and analysis. Funding for open access charge: Start-up grant from UIUC.
Conflict of interest statement. S.M.F. is an employee of Ionis Pharmaceuticals, and receives salary from the company.

REFERENCES

1. Ponting,C.P., Oliver,P.L. and Reik,W. (2009) Evolution and functions of long noncoding RNAs. *Cell*, **136**, 629–641.
2. Wang,K.C. and Chang,H.Y. (2011) Molecular mechanisms of long noncoding RNAs. *Mol. Cell*, **43**, 904–914.
3. Mercer,T.R., Dinger,M.E. and Mattick,J.S. (2009) Long non-coding RNAs: insights into functions. *Nat. Rev. Genet.*, **10**, 155–159.

4. Kitagawa,M., Kitagawa,K., Kotake,Y., Niida,H. and Ohhata,T. (2013) Cell cycle regulation by long non-coding RNAs. *Cell. Mol. Life Sci.: CMLS*, **70**, 4785–4794.
5. Sun,Q., Hao,Q. and Prasanth,K.V. (2017) Nuclear long noncoding RNAs: key regulators of gene expression. *Trends Genet.*, **34**, 142–157.
6. Prensner,J.R. and Chinnaiyan,A.M. (2011) The emergence of lncRNAs in cancer biology. *Cancer Discov.*, **1**, 391–407.
7. Batista,P.J. and Chang,H.Y. (2013) Long noncoding RNAs: cellular address codes in development and disease. *Cell*, **152**, 1298–1307.
8. Gutschner,T. and Diederichs,S. (2012) The hallmarks of cancer: a long non-coding RNA point of view. *RNA Biol.*, **9**, 703–719.
9. Gutschner,T., Hammerle,M., Eissmann,M., Hsu,J., Kim,Y., Hung,G., Revenko,A., Arun,G., Stentrup,M., Gross,M. *et al.* (2013) The noncoding RNA MALAT1 is a critical regulator of the metastasis phenotype of lung cancer cells. *Cancer Res.*, **73**, 1180–1189.
10. St Laurent,G., Wahlestedt,C. and Kapranov,P. (2015) The landscape of long noncoding RNA classification. *Trends Genet.*, **31**, 239–251.
11. Ameres,S.L. and Zamore,P.D. (2013) Diversifying microRNA sequence and function. *Nat. Rev. Mol. Cell Biol.*, **14**, 475–488.
12. Rodriguez,A., Griffiths-Jones,S., Ashurst,J.L. and Bradley,A. (2004) Identification of mammalian microRNA host genes and transcription units. *Genome Res.*, **14**, 1902–1910.
13. Berezikov,E., Chung,W.J., Willis,J., Cuppen,E. and Lai,E.C. (2007) Mammalian mirtron genes. *Mol. Cell*, **28**, 328–336.
14. Monteys,A.M., Spengler,R.M., Wan,J., Tecedor,L., Lennox,K.A., Xing,Y. and Davidson,B.L. (2010) Structure and activity of putative intronic miRNA promoters. *RNA*, **16**, 495–505.
15. Kahl,G. (2009) *The Dictionary of Genomics, Transcriptomics and Proteomics*. 5 edn. Wiley-Blackwell, Hoboken, NJ.
16. Dhir,A., Dhir,S., Proudfoot,N.J. and Jopling,C.L. (2015) Microprocessor mediates transcriptional termination of long noncoding RNA transcripts hosting microRNAs. *Nat. Struct. Mol. Biol.*, **22**, 319–327.
17. Molinari,C., Salvi,S., Foca,F., Teodorani,N., Saragoni,L., Puccetti,M., Passardi,A., Tamberi,S., Avanzolini,A., Lucci,E. *et al.* (2016) miR-17-92a-1 cluster host gene (MIR17HG) evaluation and response to neoadjuvant chemoradiotherapy in rectal cancer. *Oncol. Targets Ther.*, **9**, 2735–2742.
18. Dong,Y., Yan,W., Zhang,S.L., Zhang,M.Z., Zhou,Y.P., Ling,H.H., Ning,M., Zhao,Y., Huang,A. and Zhang,P. (2017) Prognostic values of long non-coding RNA MIR22HG for patients with hepatocellular carcinoma after hepatectomy. *Oncotarget*, **8**, 114041–114049.
19. Raveh,E., Matouk,I.J., Gilon,M. and Hochberg,A. (2015) The H19 Long non-coding RNA in cancer initiation, progression and metastasis - a proposed unifying theory. *Mol. Cancer*, **14**, 184.
20. Tseng,Y.Y., Moriarity,B.S., Gong,W., Akiyama,R., Tiwari,A., Kawakami,H., Ronning,P., Reuland,B., Guenther,K., Beadnell,T.C. *et al.* (2014) PVT1 dependence in cancer with MYC copy-number increase. *Nature*, **512**, 82–86.
21. Colombo,T., Farina,L., Macino,G. and Paci,P. (2015) PVT1: a rising star among oncogenic long noncoding RNAs. *BioMed Res. Int.*, **2015**, 304208.
22. Ng,S.Y., Bogu,G.K., Soh,B.S. and Stanton,L.W. (2013) The long noncoding RNA RMST interacts with SOX2 to regulate neurogenesis. *Mol. Cell*, **51**, 349–359.
23. Shih,J.W., Chiang,W.F., Wu,A.T.H., Wu,M.H., Wang,L.Y., Yu,Y.L., Hung,Y.W., Wang,W.C., Chu,C.Y., Hung,C.L. *et al.* (2017) Long noncoding RNA LncHIFCAR/MIR31HG is a HIF-1alpha co-activator driving oral cancer progression. *Nat. Commun.*, **8**, 15874.
24. Tripathi,V., Shen,Z., Chakraborty,A., Giri,S., Freier,S.M., Wu,X., Zhang,Y., Gorospe,M., Prasanth,S.G., Lal,A. *et al.* (2013) Long noncoding RNA MALAT1 controls cell cycle progression by regulating the expression of oncogenic transcription factor B-MYB. *PLos Genet.*, **9**, e1003368.
25. Carleton,M., Cleary,M.A. and Linsley,P.S. (2007) MicroRNAs and cell cycle regulation. *Cell Cycle*, **6**, 2127–2132.
26. Frenzel,A., Loven,J. and Henriksson,M.A. (2010) Targeting MYC-Regulated miRNAs to combat cancer. *Genes Cancer*, **1**, 660–667.
27. Roush,S. and Slack,F.J. (2008) The let-7 family of microRNAs. *Trends Cell Biol.*, **18**, 505–516.
28. Deng,L., Shang,L., Bai,S., Chen,J., He,X., Martin-Trevino,R., Chen,S., Li,X.Y., Meng,X., Yu,B. *et al.* (2014) MicroRNA100 inhibits self-renewal of breast cancer stem-like cells and breast tumor development. *Cancer Res.*, **74**, 6648–6660.
29. Kim,S.W., Ramasamy,K., Bouamar,H., Lin,A.P., Jiang,D. and Aguiar,R.C. (2012) MicroRNAs miR-125a and miR-125b constitutively activate the NF-kappaB pathway by targeting the tumor necrosis factor alpha-induced protein 3 (TNFAIP3, A20). *PNAS*, **109**, 7865–7870.
30. Zeng,C.W., Chen,Z.H., Zhang,X.J., Han,B.W., Lin,K.Y., Li,X.J., Wei,P.P., Zhang,H., Li,Y. and Chen,Y.Q. (2014) MIR125B1 represses the degradation of the PML-RARA oncoprotein by an autophagy-lysosomal pathway in acute promyelocytic leukemia. *Autophagy*, **10**, 1726–1737.
31. Zheng,Y.S., Zhang,H., Zhang,X.J., Feng,D.D., Luo,X.Q., Zeng,C.W., Lin,K.Y., Zhou,H., Qu,L.H., Zhang,P. *et al.* (2012) MiR-100 regulates cell differentiation and survival by targeting RBSP3, a phosphatase-like tumor suppressor in acute myeloid leukemia. *Oncogene*, **31**, 80–92.
32. Nagaraja,A.K., Creighton,C.J., Yu,Z., Zhu,H., Gunaratne,P.H., Reid,J.G., Olokpa,E., Itamochi,H., Ueno,N.T., Hawkins,S.M. *et al.* (2010) A link between mir-100 and FRAP1/mTOR in clear cell ovarian cancer. *Mol. Endocrinol.*, **24**, 447–463.
33. Petrelli,A., Perra,A., Schernhuber,K., Cargnelutti,M., Salvi,A., Migliore,C., Ghiso,E., Benetti,A., Barlati,S., Ledda-Columbano,G.M. *et al.* (2012) Sequential analysis of multistage hepatocarcinogenesis reveals that miR-100 and PLK1 dysregulation is an early event maintained along tumor progression. *Oncogene*, **31**, 4517–4526.
34. Hayashita,Y., Osada,H., Tatematsu,Y., Yamada,H., Yanagisawa,K., Tomida,S., Yatabe,Y., Kawahara,K., Sekido,Y. and Takahashi,T. (2005) A polycistronic microRNA cluster, miR-17-92, is overexpressed in human lung cancers and enhances cell proliferation. *Cancer Res.*, **65**, 9628–9632.
35. Lu,Y., Thomson,J.M., Wong,H.Y., Hammond,S.M. and Hogan,B.L. (2007) Transgenic over-expression of the microRNA miR-17-92 cluster promotes proliferation and inhibits differentiation of lung epithelial progenitor cells. *Dev. Biol.*, **310**, 442–453.
36. Legnini,I., Morlando,M., Mangiavacchi,A., Fatica,A. and Bozzoni,I. (2014) A feedforward regulatory loop between HuR and the long noncoding RNA linc-MD1 controls early phases of myogenesis. *Mol. Cell*, **53**, 506–514.
37. Emmrich,S., Streltsov,A., Schmidt,F., Thangapandi,V.R., Reinhardt,D. and Klusmann,J.H. (2014) LincRNAs MONC and MIR100HG act as oncogenes in acute megakaryoblastic leukemia. *Mol. Cancer*, **13**, 171.
38. Shang,C., Zhu,W., Liu,T., Wang,W., Huang,G., Huang,J., Zhao,P., Zhao,Y. and Yao,S. (2016) Characterization of long non-coding RNA expression profiles in lymph node metastasis of early-stage cervical cancer. *Oncol. Rep.*, **35**, 3185–3197.
39. Dawson,P.J., Wolman,S.R., Tait,L., Heppner,G.H. and Miller,F.R. (1996) MCF10AT: A model for the evolution of cancer from proliferative breast disease. *Am. J. Pathol.*, **148**, 313–319.
40. Santner,S.J., Dawson,P.J., Tait,L., Soule,H.D., Eliason,J., Mohamed,A.N., Wolman,S.R., Heppner,G.H. and Miller,F.R. (2001) Malignant MCF10CA1 cell lines derived from premalignant human breast epithelial MCF10AT cells. *Breast Cancer Res. Treat.*, **65**, 101–110.
41. Weiger,M.C., Vedham,V., Stuelten,C.H., Shou,K., Herrera,M., Sato,M., Losert,W. and Parent,C.A. (2013) Real-time motion analysis reveals cell directionality as an indicator of breast cancer progression. *PLoS One*, **8**, e58859.
42. Jadaliha,M., Zong,X., Malakar,P., Ray,T., Singh,D.K., Freier,S.M., Jensen,T., Prasanth,S.G., Karni,R., Ray,P.S. *et al.* (2016) Functional and prognostic significance of long non-coding RNA MALAT1 as a metastasis driver in ER negative lymph node negative breast cancer. *Oncotarget*, **7**, 40418–40436.
43. Singh,D.K., Gholamalamdari,O., Jadaliha,M., Ling Li,X., Lin,Y.C., Zhang,Y., Guang,S., Hashemikhabir,S., Tiwari,S., Zhu,Y.J. *et al.* (2017) PSIP1/p75 promotes tumorigenicity in breast cancer cells by promoting the transcription of cell cycle genes. *Carcinogenesis*, **38**, 966–975.
44. Sun,D., Lee,Y.S., Malhotra,A., Kim,H.K., Matecic,M., Evans,C., Jensen,R.V., Moskaluk,C.A. and Dutta,A. (2011) miR-99 family of MicroRNAs suppresses the expression of prostate-specific antigen and prostate cancer cell proliferation. *Cancer Res.*, **71**, 1313–1324.

45. Shi,W., Alajez,N.M., Bastianutto,C., Hui,A.B., Mocanu,J.D., Ito,E., Busson,P., Lo,K.W., Ng,R., Waldron,J. *et al.* (2010) Significance of Plk1 regulation by miR-100 in human nasopharyngeal cancer. *Int. J. Cancer*, **126**, 2036–2048.
46. Sylvius,N., Bonne,G., Straatman,K., Reddy,T., Gant,T.W. and Shackleton,S. (2011) MicroRNA expression profiling in patients with lamin A/C-associated muscular dystrophy. *FASEB J.*, **25**, 3966–3978.
47. Catto,J.W., Miah,S., Owen,H.C., Bryant,H., Myers,K., Dudziec,E., Larre,S., Milo,M., Rehman,I., Rosario,D.J. *et al.* (2009) Distinct microRNA alterations characterize high- and low-grade bladder cancer. *Cancer Res.*, **69**, 8472–8481.
48. Geisler,S. and Coller,J. (2013) RNA in unexpected places: long non-coding RNA functions in diverse cellular contexts. *Nat. Rev. Mol. Cell Biol.*, **14**, 699–712.
49. Turner,M., Galloway,A. and Vigorito,E. (2014) Noncoding RNA and its associated proteins as regulatory elements of the immune system. *Nat. Immunol.*, **15**, 484–491.
50. Guttman,M. and Rinn,J.L. (2012) Modular regulatory principles of large non-coding RNAs. *Nature*, **482**, 339–346.
51. Lopez de Silanes,I., Zhan,M., Lal,A., Yang,X. and Gorospe,M. (2004) Identification of a target RNA motif for RNA-binding protein HuR. *PNAS*, **101**, 2987–2992.
52. Lebedeva,S., Jens,M., Theil,K., Schwanhausser,B., Selbach,M., Landthaler,M. and Rajewsky,N. (2011) Transcriptome-wide analysis of regulatory interactions of the RNA-binding protein HuR. *Mol. Cell*, **43**, 340–352.
53. Mukherjee,N., Corcoran,D.L., Nusbaum,J.D., Reid,D.W., Georgiev,S., Hafner,M., Ascano,M. Jr, Tuschl,T., Ohler,U. and Keene,J.D. (2011) Integrative regulatory mapping indicates that the RNA-binding protein HuR couples pre-mRNA processing and mRNA stability. *Mol. Cell*, **43**, 327–339.
54. Heinonen,M., Fagerholm,R., Aaltonen,K., Kilpivaara,O., Aittomaki,K., Blomqvist,C., Heikkila,P., Haglund,C., Nevanlinna,H. and Ristimaki,A. (2007) Prognostic role of HuR in hereditary breast cancer. *Clin. Cancer Res.*, **13**, 6959–6963.
55. Mazan-Mamczarz,K., Galban,S., Lopez de Silanes,I., Martindale,J.L., Atasoy,U., Keene,J.D. and Gorospe,M. (2003) RNA-binding protein HuR enhances p53 translation in response to ultraviolet light irradiation. *PNAS*, **100**, 8354–8359.
56. Lopez de Silanes,I., Fan,J., Yang,X., Zonderman,A.B., Potapova,O., Pizer,E.S. and Gorospe,M. (2003) Role of the RNA-binding protein HuR in colon carcinogenesis. *Oncogene*, **22**, 7146–7154.
57. Wang,W.G., Furneaux,H., Cheng,H.M., Caldwell,M.C., Hutter,D., Liu,Y.S., Holbrook,N. and Gorospe,M. (2000) HuR regulates p21 mRNA stabilization by UV light. *Mol. Cell. Biol.*, **20**, 760–769.
58. Wang,W., Caldwell,M.C., Lin,S., Furneaux,H. and Gorospe,M. (2000) HuR regulates cyclin A and cyclin B1 mRNA stability during cell proliferation. *EMBO J.*, **19**, 2340–2350.
59. Cammas,A., Sanchez,B.J., Lian,X.J., Dormoy-Raclet,V., van der Giessen,K., Lopez de Silanes,I., Ma,J., Wilusz,C., Richardson,J., Gorospe,M. *et al.* (2014) Destabilization of nucleophosmin mRNA by the HuR/KSRP complex is required for muscle fibre formation. *Nat. Commun.*, **5**, 4190.
60. Anantharaman,A., Tripathi,V., Khan,A., Yoon,J.H., Singh,D.K., Gholamalamdari,O., Guang,S., Ohlson,J., Wahlstedt,H., Ohman,M. *et al.* (2017) ADAR2 regulates RNA stability by modifying access of decay-promoting RNA-binding proteins. *Nucleic Acids Res.*, **45**, 4189–4201.
61. Yoon,J.H., Abdelmohsen,K., Srikantan,S., Yang,X., Martindale,J.L., De,S., Huarte,M., Zhan,M., Becker,K.G. and Gorospe,M. (2012) LincRNA-p21 suppresses target mRNA translation. *Mol. Cell*, **47**, 648–655.
62. Abdelmohsen,K. and Gorospe,M. (2010) Posttranscriptional regulation of cancer traits by HuR. *Wiley Interdiscip. Rev. RNA*, **1**, 214–229.
63. Abdelmohsen,K., Panda,A.C., Kang,M.J., Guo,R., Kim,J., Grammatikakis,I., Yoon,J.H., Dudekula,D.B., Noh,J.H., Yang,X. *et al.* (2014) 7SL RNA represses p53 translation by competing with HuR. *Nucleic Acids Res.*, **42**, 10099–10111.
64. Brennan,C.M. and Steitz,J.A. (2001) HuR and mRNA stability. *Cell. Mol. Life Sci.*, **58**, 266–277.
65. Kundu,P., Fabian,M.R., Sonenberg,N., Bhattacharyya,S.N. and Filipowicz,W. (2012) HuR protein attenuates miRNA-mediated repression by promoting miRISC dissociation from the target RNA. *Nucleic Acids Res.*, **40**, 5088–5100.
66. Kim,J., Abdelmohsen,K., Yang,X., De,S., Grammatikakis,I., Noh,J.H. and Gorospe,M. (2016) LncRNA OIP5-AS1/cyrano sponges RNA-binding protein HuR. *Nucleic Acids Res.*, **44**, 2378–2392.
67. Cao,C., Sun,J., Zhang,D., Guo,X., Xie,L., Li,X., Wu,D. and Liu,L. (2015) The long intergenic noncoding RNA UFC1, a target of MicroRNA 34a, interacts with the mRNA stabilizing protein HuR to increase levels of beta-catenin in HCC cells. *Gastroenterology*, **148**, 415–426.
68. Yoon,J.H., Abdelmohsen,K., Kim,J., Yang,X., Martindale,J.L., Tominaga-Yamanaka,K., White,E.J., Orjalo,A.V., Rinn,J.L., Kreft,S.G. *et al.* (2013) Scaffold function of long non-coding RNA HOTAIR in protein ubiquitination. *Nat. Commun.*, **4**, 2939.
69. Kim,H.H., Kuwano,Y., Srikantan,S., Lee,E.K., Martindale,J.L. and Gorospe,M. (2009) HuR recruits let-7/RISC to repress c-Myc expression. *Genes Dev.*, **23**, 1743–1748.
70. Chang,N., Yi,J., Guo,G., Liu,X., Shang,Y., Tong,T., Cui,Q., Zhan,M., Gorospe,M. and Wang,W. (2010) HuR uses AUF1 as a cofactor to promote p16INK4 mRNA decay. *Mol. Cell. Biol.*, **30**, 3875–3886.
71. Kim,H.H., Yang,X., Kuwano,Y. and Gorospe,M. (2008) Modification at HuR(S242) alters HuR localization and proliferative influence. *Cell Cycle*, **7**, 3371–3377.
72. Kim,H.H. and Gorospe,M. (2008) Phosphorylated HuR shuttles in cycles. *Cell Cycle*, **7**, 3124–3126.